

ON He BUBBLES IN NEUTRON IRRADIATED SYLRAMIC™ TYPE SiC FIBERS—D. S. Gelles and G. E. Youngblood (Pacific Northwest National Laboratory)*

OBJECTIVE

The objective of this effort is to improve understanding of the effects of helium when it is produced in SiC/SiC composites during neutron irradiation in a fusion environment.

SUMMARY

Sylramic™ type SiC fibers, which contain at least 2.3 wt% B, were examined by TEM following neutron irradiation to dose levels of ~ 7 dpa in HFIR at 800°C and to ~ 1 dpa in ATR at 1090°C. At these radiation damage dose levels, transmutation of the boron-10 component effectively “dopes” the Sylramic™ type fibers with up to 10,000 appm helium. Following irradiation at 800°C, bubble development was too fine to resolve even by high resolution TEM. However, following irradiation at 1090°C helium bubble development was resolvable, but complex. A fine dispersion of 1-nm bubbles was observed within the SiC grains and a coarse, non-uniform distribution of irregular 25-nm bubbles was observed on grain boundaries. In addition, some unusual arrays of planar 2.5-nm thick bubbles were observed in the SiC grains and equiaxed bubbles were observed in the boride precipitate particles contained within the fiber microstructure. Not unexpectedly, helium retention and bubble formation in β-SiC depends on details of the polycrystalline microstructure as well as the irradiation conditions.

PROGRESS AND STATUS

Introduction

In a fusion reactor with SiC/SiC composite components, large levels of hydrogen and helium will be generated by transmutation of SiC. For instance, in an ARIES-IV first wall with a fast flux ($E > 0.1$ MeV) of 1.9×10^{19} m²/s Heinisch predicts transmutation production ratios of 58 appm H/dpa and 161 ppm He/dpa for the C and Si components, respectively [1]. At those production rates, after one year the He concentration in SiC could be > 6000 appm in some regions. Since helium is insoluble in SiC, in the point-defect accumulation regime (at temperatures lower than ~ 800°C) swelling is enhanced by the additional accumulation of mostly small clusters of interstitial helium. At higher temperatures the helium clusters begin to coalesce (> 900°C), and are trapped by irradiation-induced vacancies. Together with irradiation-induced point defects, helium in the lattice is expected to degrade the thermal conductivity. At even higher temperatures when the vacancies become mobile (> 1000–1100°C in SiC), the helium is expected to stabilize vacancy clusters to form He-filled bubbles. Such helium-filled bubbles in SiC are expected to degrade mechanical properties. The degradation could be especially severe if the bubbles tend to orient and/or align along common layers such as grain boundaries or faulted planes.

Helium effects in metals and, in general, in other polycrystalline materials (including He diffusion and bubble nucleation under irradiation, dissociation at high temperatures, homogeneous nucleation in the bulk vs. heterogeneous nucleation at extended defects, bubble coarsening and coalescence, bubble pressure state, formation and growth of He platelets as well as possible effects on mechanical properties) are reviewed in Ref. [2]. Extensive single-, dual-, and or triple-beam accelerator irradiation experiments have been performed on SiC or SiC/SiC composites to examine synergistic radiation damage-helium and radiation damage-helium/hydrogen effects [3–5]. In particular, for fusion relevant helium-to-dpa ratios, Katoh observed significantly enhanced swelling in the 400–800°C temperature range for dual beam irradiations with 5.1 MeV Si⁺²-ion and energy degraded 1.0 MeV He⁺-ions [6]. However, for $T > \sim 900^\circ\text{C}$ similar saturated swelling levels both with and without helium co-implantation suggested a modification of the defect structure. The swelling for dual beam irradiation is greater than

*Pacific Northwest National Laboratory (PNNL) is operated for the U.S. Department of Energy by Battelle Memorial Institute under contract DE-AC06-76RLO-1830.

for neutron irradiations at comparable conditions, except that damage rates are on the order of 10^3 greater for the dual beam tests. Recent work by Chen et al. demonstrated that helium implantation to 2450 appm at ambient temperature produced platelets on the order of 10 nm in diameter lying on (0001) habit planes in hot-pressed hexagonal phase α -SiC [8,9]. Upon annealing to $\sim 1500\text{K}$, the platelets disintegrated into discs of bubbles as the Si and C atoms became mobile. A question that arose was whether similar bubble geometries or preferred locations would develop in β -SiC or, in particular, in fibers with primarily polycrystalline, cubic β -phase SiC grains that contain numerous faulted planes.

Several types of SiC fibers were irradiated at 800°C in the High Flux Isotope Reactor (HFIR) at Oak Ridge National Laboratory and at 1090°C in the Advanced Test Reactor (ATR) at Idaho Falls. One of the fiber types was Sylramic™, which contains a significant amount of boron doping. As boron can transmute to helium and lithium following capture of a low energy neutron, irradiated Sylramic™ fibers provide the opportunity to study effects of He production on SiC microstructures. However, such studies must be performed with the understanding that Li is also produced and that He and Li accumulate in separate spherical halo-like distributions around boride precipitate particles when the boron undergoes transmutation [10,11]. As in the accelerator experiments, the helium production rates during such “boron/helium-doping” experiments are expected to be orders of magnitude higher than for the helium production rates from Si and C transmutation in a fusion neutron energy spectrum. Furthermore, the He and Li recoil atoms themselves are energetic enough to contribute significantly to the overall radiation damage.

This report presents a detailed search by transmission electron microscopy (TEM) for helium bubbles in the boron-containing Sylramic™ type SiC fibers irradiated at 800 and 1090°C and, if formed, a microstructure examination of these bubbles.

Experimental Procedure

The composition of commercial Sylramic™ fiber in wt% is: Si (66.6), C (28.5), B (2.3), Ti (2.1), O (0.8), and N (0.4). Typical properties are: tensile strength (3.2 MPa), elastic modulus (380 GPa), diameter (10 μm), bulk density (3.0+ g/cc), C/Si ratio (1/1), and thermal conductivity at 323K (40–46 W/mK). The high degree of crystallinity and density lead to a high elastic modulus and thermal conductivity for this SiC fiber. The small diameter and relatively fine grain size allow this fiber to be readily woven into fabrics for composite 2D- or 3D-structures. Furthermore, the Sylramic™ fiber is thermally and chemically stable under ceramic matrix composite processing conditions up to $\sim 1800^\circ\text{C}$. Developed by Dow Corning Corporation with support from NASA, Sylramic™ is primarily stoichiometric polycrystalline β -SiC. The 2.3 wt% boron exists primarily as crystalline precipitates of titanium diboride. The $\sim 40\text{-nm}$ TiB_2 crystallites are uniformly distributed and typically are found at triple points of the 100–500 nm sized β -SiC grains [12]. The latter contains considerable twinning and stacking faults, primarily with {111} habit planes. Small amounts of B_4C (1 wt%) and BN also occur. The TiB_2 , as well as minor amounts of B_4C and BN, limit grain growth during sintering of the green fiber.

Individual 50-mm long Sylramic™ SiC tows were encapsulated within Hexoloy™ sintered α -SiC protection tubes. Small vent holes in the tubes allowed gas exchange with the surrounding helium atmosphere. The specimens were irradiated in the HFIR as part of the HFIR-MFE-RB-14J experiment at 800°C (7.0 dpa) [13] or in the ATR as part of a similar experiment called “KAMET” at 1090°C (0.65 dpa) [14].

The transmutation of B proceeds as follows [15]. Natural He boron contains $\sim 20\%$ ^{10}B which can absorb a low energy neutron and transmute to ^7Li while releasing a α -particle. For 94% of the time, the ^7Li is in an excited state with recoil kinetic energy 0.840 MeV and the He atom recoils with a kinetic energy of 1.47 MeV. For the remaining 6% of the time, these atoms recoil with kinetic energies of 1.015 and 1.777 MeV, respectively. Stopping and Range of Ions in Matter (SRIM) calculations [16] for these conditions in SiC are given in Table 1.

Table 1 indicates that the bulk of the helium produced by transmutation will be deposited in a spherical halo about 3.4 μm from a $\sim 40\text{-nm}$ TiB_2 particle with typical spacing between particles of 100–200 nm. Thus, the He (and Li) haloes formed about each TiB_2 particle contain $\sim 10^5$ other halo sources, and the overall He (and Li) deposition is expected to be fairly uniform within the SiC lattice. As mentioned, the relatively high recoil atom kinetic energies significantly contribute to the overall point-defect production in the fibers as well.

Table 1. SRIM calculations for Range and Straggle as a function of ion kinetic energy in SiC

Ion	Energy (MeV)	Fraction (%)	Range (μm)	Straggle (nm)
He	1.47	94	3.36	116
He	1.78	6	4.12	124
Li	0.84	94	1.79	110
Li	1.01	6	2.33	114

The helium content for the fiber specimens was determined by isotope-dilution gas mass spectroscopy (IDGMS) following vaporization in a resistance-heated graphite crucible. This method, developed to accurately measure low levels of helium in small liquid or solid samples, measures the absolute amount of ^4He released relative to a known quantity of added ^3He [17].

The $\sim 10\ \mu\text{m}$ diameter fibers were successfully thinned for electron microscopy by ion milling in a Precision Ion Polishing System (PIPS) from Gatan, Inc., operating with 5 KeV argon ions. A few fibers were glued between Mo washers using thermal setting epoxy, and then ion-milled in double modulation mode with the ion beam parallel to the fiber direction. This milling geometry tended to produce an elliptical cross-section from the circular fibers. It was found during preliminary preparation tests on unirradiated fibers that individual fibers were electron transparent when milled through to separation, but fiber vibration during examination prevented observation with high resolution. However, where fibers crossed, milling was sufficient to provide electron transparent regions without separation, and such regions could be examined at high resolution. Microstructure examinations by TEM were performed on a JEM 2010F operating at 200 KeV equipped with a Gatan parallel electron energy loss spectrometer (EELS) and an Oxford Instruments, Inc., X-ray spectrometer with INCA software.

Results

The helium concentrations of the Sylramic™ type SiC fibers and a monolithic sintered $\alpha\text{-SiC}$ (Hexoloy™ SA) are given in Table 2.

Table 2. Helium concentration in neutron irradiated SiC materials measured by IDGMS

Sample	Condition	Mass (mg) ^a	Meas. ^4He ^b	^4He Conc. (appm) ^c
J22	Unirradiated	1.412	0.073	0.34
Hexoloy™	800°C/7.0 dpa	0.694 ^d	2.842 ^d	1,350 ^d
J22B,C	800°C/7.0 dpa	0.438 ^d	7.566 ^d	5,516 ^d
KA44rA	500°C/0.95 dpa	1.116	34.06	10,040
KA44rB,C	“ “	0.166 ^d	5.03 ^d	9,946 ^d
KA44rA	1090°C/0.65 dpa	0.842	27.66	10,810
KA44rB,C	“ “	0.155 ^d	5.04 ^d	9,982 ^d

^aMass of specimen for analysis with uncertainty ± 0.002 mg.

^bMeasured quantity of helium ($\times 10^{16}$ atoms) with uncertainty of $\pm 1\%$.

^cHelium concentration in atomic parts per million (appm) with respect to 3.04×10^{22} atoms/gm for SiC.

^dAverage values for duplicate samples B and C determined six years post-irradiation.

Samples labeled J22 were commercially available Sylramic™ fiber whereas samples labeled KA44 were a developmental version called Dow EPM. Helium contents in samples J22, KA44rA, and KA44rA were originally analyzed in 1999. Helium contents in the remaining duplicate samples were analyzed in 2005. For the complete burn-up of the 20% ^{10}B component in Sylramic™ containing 2.3 wt% natural boron, 8330 appm helium should be produced. The sintered monolithic Hexoloy sample contains 0.6 wt% natural boron (as B_4C precipitates); therefore about 2170 appm helium should be produced for complete burn-up of ^{10}B .

By examining the data in Table 2, three conclusions can be reached regarding the helium contents remaining in the irradiated fibers. First, the KA44 fibers (Dow EPM irradiated at either 500 or 1090°C) retained helium contents ~ 20% in excess of the calculated 8330 appm for complete burn-up of the boron in Sylramic™ fiber. This suggests that the assumed boron content of 2.3 wt% in the Dow EPM (developmental Sylramic™) fiber was too low. Second, the similar helium contents determined for each irradiation temperature suggests that the produced helium is a saturation value even for doses of 0.65 dpa; and that no helium was lost at the higher irradiation temperature of 1090°C. Furthermore, the helium content values determined after storage of the fibers for six years decreased by only ~ 5% which suggests that the helium was retained within the irradiated fiber microstructure in a rather stable form. This may not be the case for the irradiated J22 (commercial Sylramic™) fiber where the measured helium contents are high, but nevertheless are about 34% less than the expected saturation value for complete ^{10}B burn-up. Regardless, there is sufficient helium in all of the irradiated fibers to carry out the main objective of this study, i.e., to examine the formation, distribution, and shape of helium bubbles formed in neutron irradiated polycrystalline SiC fibers with primarily β -SiC grains.

Microstructure of unirradiated Sylramic™ fiber

The microstructure of a commercial Sylramic™ fiber sample is shown in Fig. 1. It is polycrystalline, with a grain size greater than 100 nm and exhibits a twinned structure. Composition maps for this region showing outputs for B, C, Si, Ti, O, and a background signal that provides a measure of mass or thickness variation are shown in Fig. 2. The small particles rich in Ti do not account for all regions low in Si. However, the Ti rich regions account for regions of enhanced mass or thickness, and an association with O is indicated. Unfortunately, the B and C maps contain little information due to the low energy peaks associated with these elements. However, EELS examination did show B associated with regions containing high Ti, verifying the presence of TiB_2 .

800°C irradiation

Following irradiation at 800°C, evidence for helium accumulation could not be identified. Examples at sufficient magnification to see 1-nm bubbles are given in Fig. 3, with no clear evidence for bubbles. In both examples, the image is under-focused at ~ 500 nm so that bubbles should show white with a black outline. Composition maps were generated similar to those shown in Fig. 2. A mosaic was made to identify large TiB_2 particles in thin areas at the edge of the sample and regions ~ 3 μm from the largest particles were examined in detail, without improved success at imaging He bubbles. Apparently, the helium is distributed on too fine a scale for successful bubble imaging after the 800°C irradiation.

1090°C irradiation

Following irradiation at 1090°C, bubbles were present in

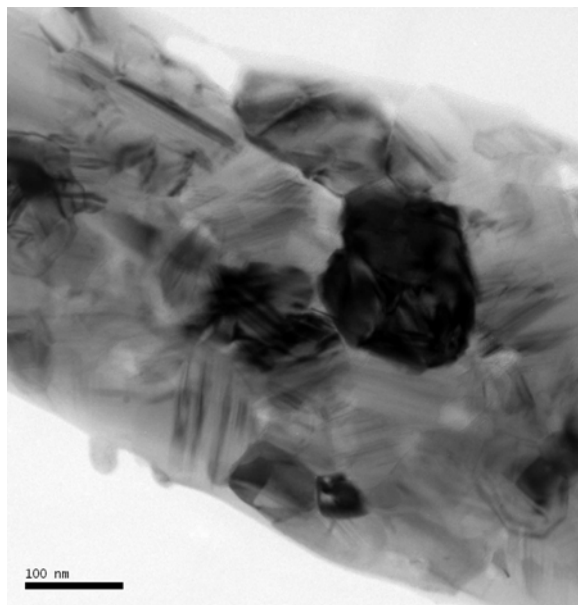


Fig. 1. An unirradiated Sylramic™ fiber thinned by ion milling.

two forms: uniformly distributed small bubbles at high density and non-uniformly distributed larger bubbles at low density. Low magnification examples of the general microstructure are provided in Fig. 4 where large bubbles on the order of 25 nm in diameter appear to be associated with grain boundaries. However, bubble shapes often are unusual, characteristically becoming pits after being distorted during preparation due to association with foil surfaces.

Examples of bubble structures at higher magnification are given in Fig. 5(a-d). Figure 5a is an under-focused image at high magnification showing a high density of small white bubbles with bubble diameters of ~ 1 nm. Figures 5b, c, and d show more complex, larger bubbles, apparently associated with grain structure of a different character. However, the fine bubbles away from the regions with complex structure are visible in the under-focused condition in Fig. 5c and in the over-focused condition in Fig. 5b. Several examples of complex bubbles were examined in stereo, which confirmed that these structures were captured within the SiC fiber and were not surface artifacts. The bubbles shown at the particle interface in Fig. 5b are of complex shape, and the bubbles in Figs. 5c and 5d appear to be planar bubbles with at least two configurations. Figure 5c shows the specimen tilted so that bubbles in the center of the array are on edge, which is an indication that these bubbles are as thin as 2.5 nm. Therefore, within the crystalline grains of Dow EPM fibers helium bubbles are formed on a very fine scale, (~ 1 nm) and are barely resolvable after irradiation at 1090°C. However, bubble accumulation at grain boundaries often develops as large as 25 nm. Bubble structure characteristic of planar bubbles in α -SiC are also found. Attempts to demonstrate that planar bubble arrays were in fact in grains of β -SiC were unsuccessful, and in one case were found to be present in a B₄C grain.

Discussion

The results of this study indicate that relatively large quantities (up to 10,000 appm) of helium were distributed on a very fine scale after neutron irradiation of boron-doped Sylramic™-type SiC fibers. Following irradiation at 800°C, bubbles could not be resolved. Following irradiation at 1090°C, bubbles could be resolved at high magnification but within the SiC grains they were only about 1 nm in diameter. However, much larger bubbles (up to 25 nm in diameter) were discovered at grain boundaries.

The large complex planar bubble arrays shown in Figs. 5c and d are not expected to be representative of β -SiC. It is more likely that they are associated with the boride additions, as demonstrated by one example where such bubbles were found to be within a B₄C grain.

The present work on bubbles in Sylramic™ type fibers can be compared with earlier work on dense, pressureless sintered monolithic Hexoloy™ SA with equiaxed grains of 4–6 μ m in diameter of hexagonal phase α -SiC [14]. Hexoloy™ SA contains less natural boron than the Sylramic-type fibers (0.6 wt% B added as B₄C to aid sintering). The present KA44 Dow EPM fibers with about four times as much boron as in Hexoloy, also generated about four times more helium than did the Hexoloy when the two materials were irradiated side-by-side in the same experiment (see Table 2). Nevertheless, the Hexoloy™ material exhibited a well-developed, dense array of 50-nm bubbles uniformly decorating grain boundaries. The bubbles were hexagonal in cross section and quite flat. So, relatively large bubbles were formed on the grain boundaries of both SiC materials, but the bubbles were larger, more densely packed and appeared only on the grain boundaries in the Hexoloy™ α -SiC. This evidence suggests that helium is trapped and dispersed on a much finer scale in the fine-grained, Sylramic™ fibers with faulted β -SiC grains as compared to the much larger-grained Hexoloy™ α -SiC with a limited fault microstructure.

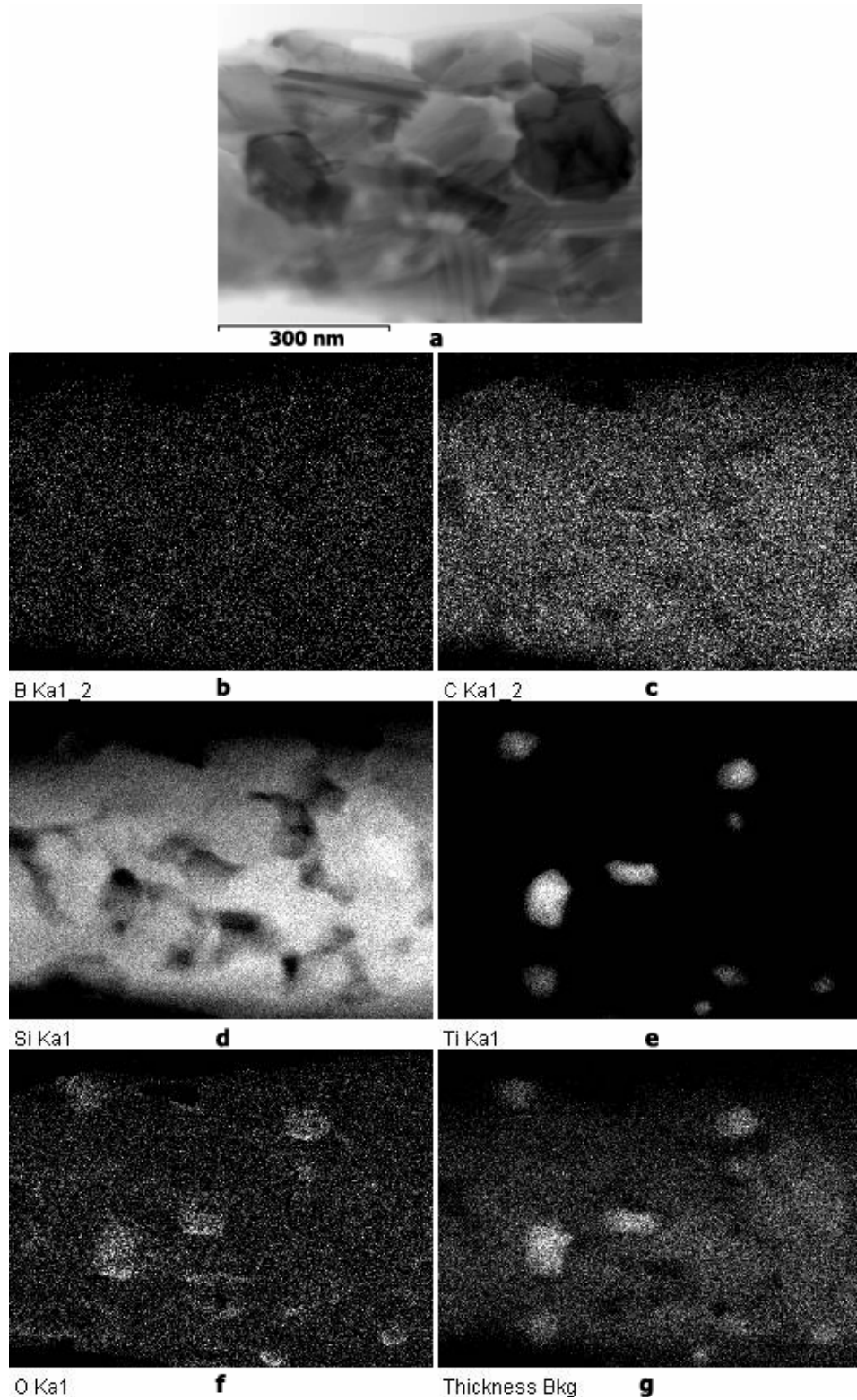


Fig. 2. Composition maps for Sylramic™ fiber showing a region of interest and B, C, Si, Ti, and O windows as well as a background window effectively mapping mass or thickness.

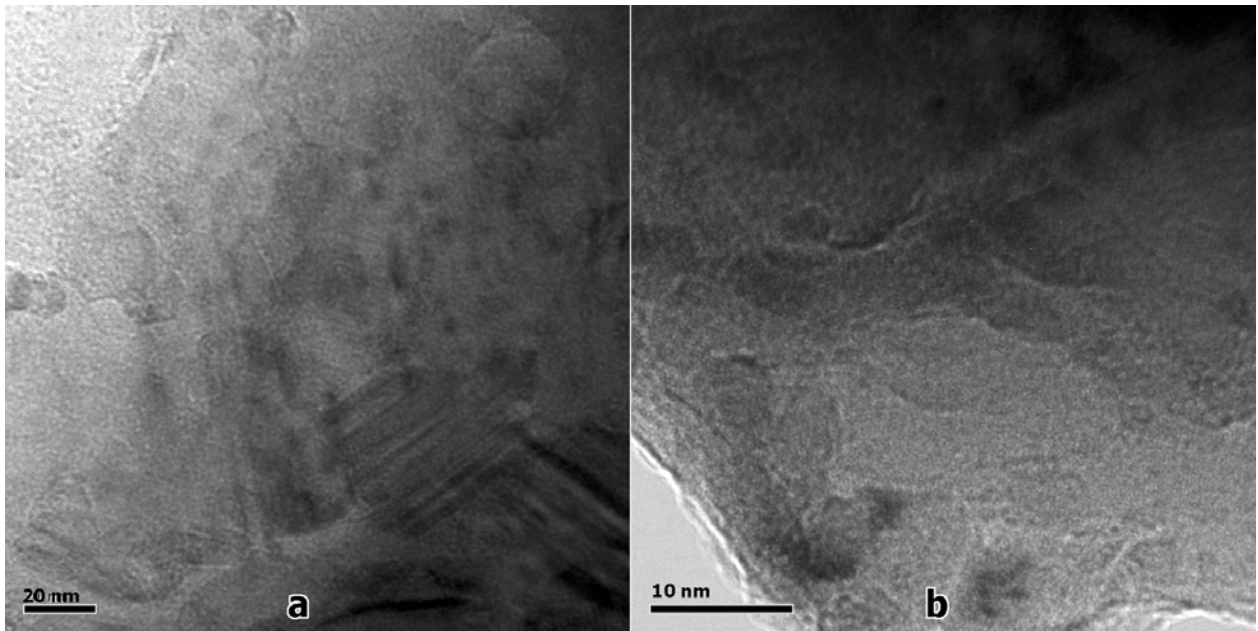


Fig. 3. Examples of microstructure in a Sylramic™ fiber at high magnification following irradiation at 800°C illustrating an unsuccessful attempt to identify fine helium bubbles.

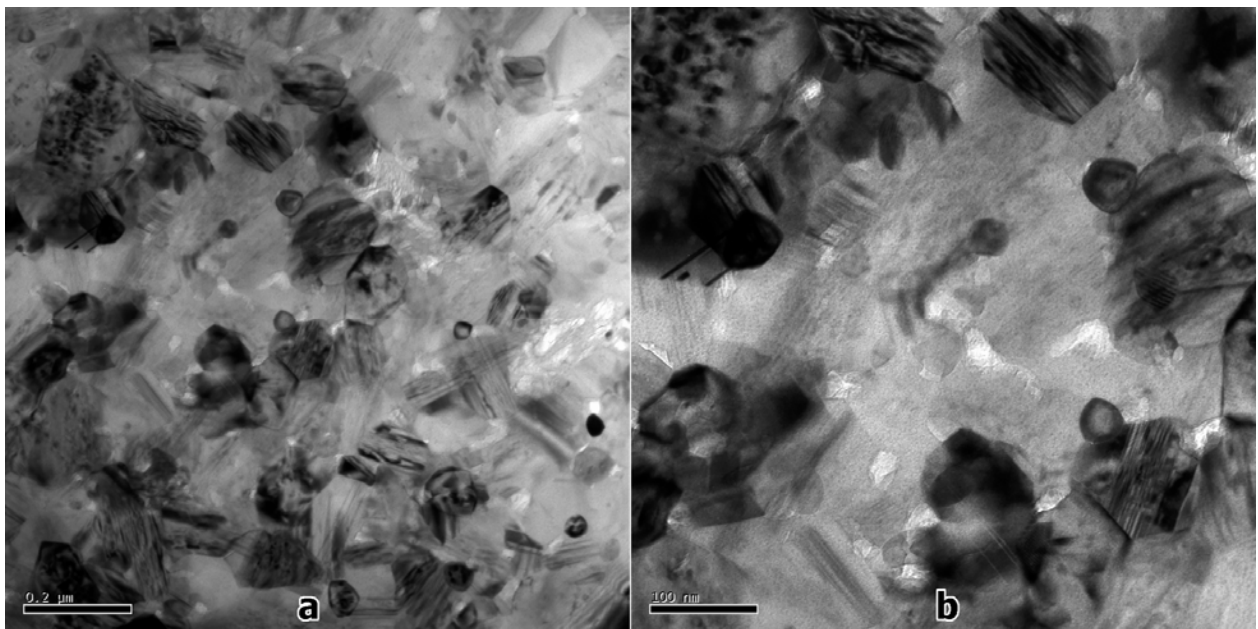


Fig. 4. Dow EPM (Sylramic™ type) fibers at low magnification following irradiation at 1090°C showing coarse helium bubble structure associated with grain boundaries and second phase particles.

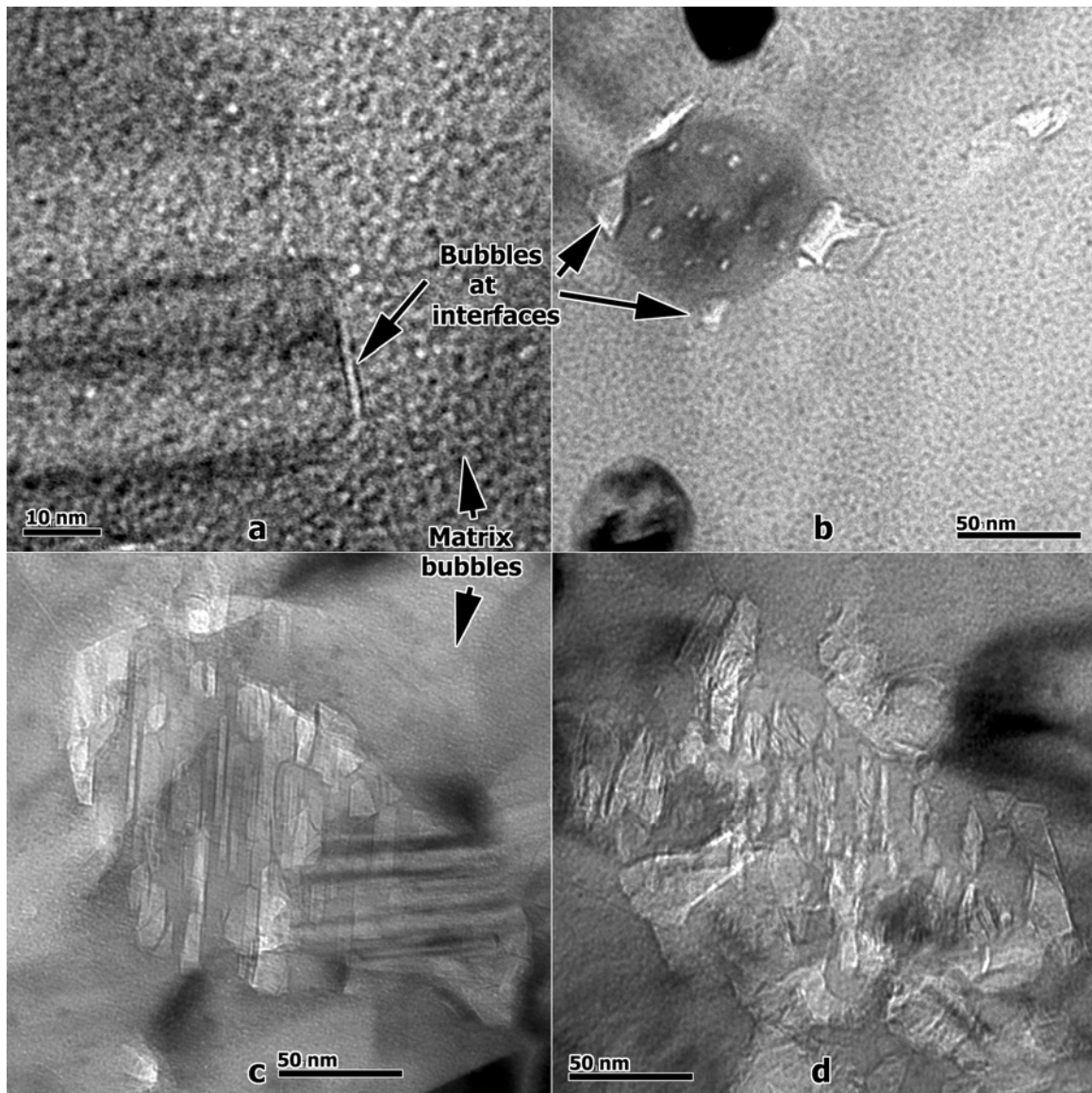


Fig. 5. Bubbles in the Dow EPM (Sylramic™ type) SiC fibers at higher magnification following irradiation at 1090°C showing bubble structures.

Ozawa et al. examined the microstructural evolution of SiC/SiC composites (made with Tyranno™-SA fiber reinforcement) using TEM after Si²⁺ with/without He⁺ ion irradiation at 1273/1673K [18]. In the dual-ion irradiations at 1673K (100 dpa, 60 appm He/dpa), helium bubbles ($d < 5\text{nm}$) were densely formed on {111} faulted planes in the fiber and in the chemical vapor infiltrated (CVI) SiC matrix. Furthermore, lens-shaped cavities (major diameter 20–50 nm) were formed on grain boundaries of the matrix. Although the experiments by Ozawa were carried out at higher irradiation temperature and with dual ion bombardment, the similar helium bubble evolutions exhibited by Sylramic™-type SiC fibers Tyranno™ to the SA is striking.

Conclusions

The effect of helium production from boron additions has been studied in Sylramic™ type SiC fibers neutron irradiated at 800 and 1090°C. It was found that polycrystalline β -SiC may absorb He on a fine scale so that bubbles are too small to resolve following irradiation at 800°C and is only ~ 1 nm in diameter in the matrix following irradiation at 1090°C. However, some larger bubbles are found at grain boundaries and sometimes within the TiB₂ particles following irradiation at 1090°C. Nevertheless, the fine dispersion of a considerable amount of helium throughout the β -SiC grains with a highly faulted microstructure indicates that β -SiC may be uniquely able to survive the high levels of helium expected to be generated in SiC in a fusion environment.

Future Work

The effort will be continued as opportunities become available.

Acknowledgements

B. M. Oliver at PNNL provided the helium analysis of the SiC materials.

References

- [1] H. L. Heinisch, Fusion Materials Semiannual Progress Report for Period Ending June 30, 2000, DOE/ER-0313/28, p. 98.
- [2] H. Trinkhaus and B. N. Singh, J. Nucl. Mater. 323 (2003) 229.
- [3] S. Nogami et al., J. Nucl. Mater. 283–287 (2000) 268.
- [4] T. Taguchi et al., J. Nucl. Mater. 307–311 (2002) 1135.
- [5] A. Hasegawa et al., J. Nucl. Mater. 329–333 (2004) 582.
- [6] Y. Katoh, H. Kishimoto, and A. Kohyama, J. Nucl. Mater. 307–311 (2002) 1221.
- [7] H. Kishimoto et al., Ceram. Trans. 144 (2002) 343–352.
- [8] J. Chen, P. Jung, and H. Trinkhaus, Phys. Rev. Letters 82 (1999) 2709.
- [9] J. Chen, P. Jung, and H. Trinkhaus, Phys. Rev. B 61 (2000) 12923.
- [10] D. S. Gelles and F. A. Garner, J. Nucl. Mater. 85–86 (1979) 689.
- [10] A. Kumar and F. A. Garner, Radiat. Effects 82 (1984) 61.
- [11] J. Lipowitz, J. A. Rabe, A. Zangvil, and Y. Xu, Ceram. Eng. Sci. Proc. 18:3 (1997) 147.
- [12] A. L. Qualls, DOE/ER-0313/28 (2000) 241.
- [13] D. J. Senior, G. E. Youngblood, L. R. Greenwood, D. V. Archer, D. L. Alexander, M. C. Chen, and G. A. Newsome, J. Nucl. Mater. 317 (2003) 145.
- [14] B. A. Oliver, private communication.
- [15] G. R. Greenwood, private communication.
- [16] H. Farrar and B. M. Oliver, J. Vac. Sci. Technol. A4 (1986) 1740.
- [17] K. Ozawa, S. Kondo, T. Hinoki, K. Jimbo, and A. Kohyama, Fusion Sci. Technol. 47 (2005) 871.